CrossMark

ORIGINAL ARTICLE

The ratio between corner frequencies of source spectra of *P*- and *S*-waves—a new discriminant between earthquakes and quarry blasts

G. Ataeva · Y. Gitterman · A. Shapira

Abstract This study analyzes and compares the *P*- and *S*-wave displacement spectra from local earthquakes and explosions of similar magnitudes. We propose a new approach to discrimination between low-magnitude shallow earthquakes and explosions by using ratios of *P*- to *S*-wave corner frequencies as a criterion. We have explored 2430 digital records of the Israeli Seismic Network (ISN) from 456 local events (226 earthquakes, 230 quarry blasts, and a few underwater explosions) of magnitudes $Md = 1.4$–3.4, which occurred at distances up to 250 km during 2001–2013 years. *P*-wave and *S*-wave displacement spectra were computed for all events following Brune's source model of earthquakes (1970, 1971) and applying the distance correction coefficients (Shapira and Hofstetter, Teconophysics 217:217–226, 1993; Ataeva G, Shapira A, Hofstetter A, J Seismol 19:389-401, 2015), The corner frequencies and moment magnitudes were determined using multiple stations for each event, and then the comparative analysis was performed.

The analysis showed that both *P*-wave and especially *S*-wave displacement spectra of quarry blasts demonstrate the corner frequencies lower than those obtained from earthquakes of similar magnitudes. A clear separation between earthquake and explosion populations was obtained for ratios of *P*- to *S*-wave corner frequency $f_0(P)/f_0(S)$. The ratios were computed for each event with corner frequencies f_0 of *P*- and *S*-wave, which were obtained from the measured f_0^i at individual stations, then corrected for distance and finally averaged. We obtained empirically the average estimation of $f_0(P)/f_0(S) = 1.23$ for all used earthquakes, and 1.86 for all explosions. We found that the difference in the ratios can be an effective discrimination parameter which does not depend on estimated moment magnitude M_w.

The new multi-station Corner Frequency Discriminant (*CFD*) for earthquakes and explosions in Israel was developed based on ratios *P*- to *S*-wave corner frequencies $f_0(P)/f_0(S)$, with the empirical threshold value of the ratio for Israel as 1.48.

1 Introduction

The problem of discriminating between man-made explosions and natural earthquakes is an important issue in seismic monitoring. In spite of many efforts over several decades, the discrimination of small magnitude events is still a difficult problem. A variety of waveform-based methods have been studied including ratios between amplitudes of different seismic phases (e.g., Bennett and Murphy, 1986; Wuster 1993; Plafcan et al. 1997; McLaughlin et al., 2004, Morozov, 2008, Anderson

G. Ataeva (✉) · Y. Gitterman
Geophysical Institute of Israel, Lod, Israel
e-mail: galinaa@gii.co.il

A. Shapira
National Steering Committee for Earthquake Preparedness, Jerusalem, Israel

⚊ Springer

et al., 2009), analysis of the velocity spectra (e.g., Taylor et al., 1988; Kim et al. 1993, 1994; Walter et al., 1995; Gitterman et al., 1998), analysis of coda waves (e.g., Su et al., 1991; Hartse et al., 1995) and detection of ripple-firing spectral modulation (e.g., Hedlin et al., 1990; Gitterman and van Eck, 1993; Smith, 1993; Carr and Garbin, 1998; Arrowsmith et al. 2006, 2007).

One of the main spectral features, proposed for identification of quarry blasts conducted by the ripple-firing technology, is the spectral modulation, similar at different network stations and not presented in earthquake velocity spectra (Gitterman and van Eck, 1993). It was also observed in Israel that seismograms of explosions are richer in low-frequency energy as compared to earthquakes, either because of higher attenuation of high-frequency seismic waves or the efficient wave interference during generating surface waves, or both (Gitterman et al., 1998). These effects were utilized in a multi-station spectral discrimination method based on energy spectral ratio (R_E) between the low-frequency (1–3 Hz) and high-frequency (6–8 Hz) bands, and the semblance of signal spectral shapes at different stations (Gitterman et al., 1998).

It is known that source spectra of earthquakes and explosions show significant differences, due to the different source mechanisms. Explosions release their energy in a 3D symmetric volume and their waveforms are dominated by P-waves. Quarry blasts are commonly fired with a series of delays (ripple firing) in order to control the movement of rock masses during the blast. In contrast, earthquakes represent a line source, with a dimension several times larger than explosion sources and generate much larger S-waves (Wyss, and Hanks, 1971, Chapman, 2008, Shearer and Allmann, 2007, Allmann et al., 2008, Dahy and Hassib 2010). The classical source model of Brune (1970, 1971) is a theoretical representation of the source spectrum of earthquakes. Wyss and Hanks (1971) pointed the differences between P-wave displacement spectra of underground explosions and shallow earthquakes of similar body-wave magnitude. It was demonstrated that in southern California, the best earthquake/explosion discriminator is the RMS misfit between P-wave spectra and the theoretical earthquake source model (Shearer and Allmann, 2007, Allmann et al., 2008). Quarry blast spectra show a steeper fall-off at high frequencies for all magnitudes and do not fit well to the standard source model. The deficiency of high frequency seismic energy from explosions was explained by ripple-firing and/or

strong near-surface attenuation (Shearer and Allmann, 2007, Allmann et al., 2008). In other studies, enrichment of low frequency energy content for explosions has been pointed out, e.g., Taylor et al. (1988), Bennett and Murphy (1986), Su et al. (1991).

We have investigated earthquake and explosion source parameters from P- and S-wave displacement spectra, focusing on the corner frequency f_0, and demonstrated the effectiveness of the P- to S-wave corner frequencies ratio $f_0(P)/f_0(S)$ as a new multi-station discriminant between small-magnitude shallow earthquakes and explosions in terms of spectral properties.

We propose the following formulation of the Corner Frequency Discriminant (CFD), which includes (1) estimations of all corner frequencies at individual stations for an event from P- and S-waves, (2) correction of these frequencies for distance, and then (3) computation of the discriminant with the averaged multi-station values $f_0(P)$ and $f_0(S)$:

$$CFD = f_0(P) \Big/ f_0(S),$$

where $f_0 = f(f_{01}, f_{02...}f_{0n}) = \sqrt[n]{f_{01} \times f_{02} \cdots \times f_{0n}}$—the geometrical mean of corner frequencies of P- or S-waves from n stations for an event,

$f_{0i} = f_0^{\mathrm{I}} e^{\gamma R}$—corner frequency from an individual station i, corrected for distance R (Shapira and Hofstetter 1993 and Ataeva et al., 2015),

f_0^{I}—corner frequency observed at individual station i,

γ—the empirical coefficient.

The CFD, determined as ratio of corner frequencies, provided quite robust results for the data in Israel.

2 Data

In this study, we explored 2430 seismograms of 226 earthquakes and 230 explosions (quarry blasts and a few of underwater explosions occurred off-coast Israel and Lebanon) of magnitudes $Md = 1.4$–3.4 with epicentral distances up to 250 km (Fig. 1a). Most of quarry blasts were known (independently of seismic means) from monthly reports sent by the quarries to the Geophysical Institute of Israel. In some cases, quarry blasts are identified by microphone sensors presented in stations of Israel Seismic Network (ISN) that register specific explosion acoustic phases at close distances. We have tried to keep up a balance through the same magnitude ranges for earthquakes and explosions for a reliable statistical
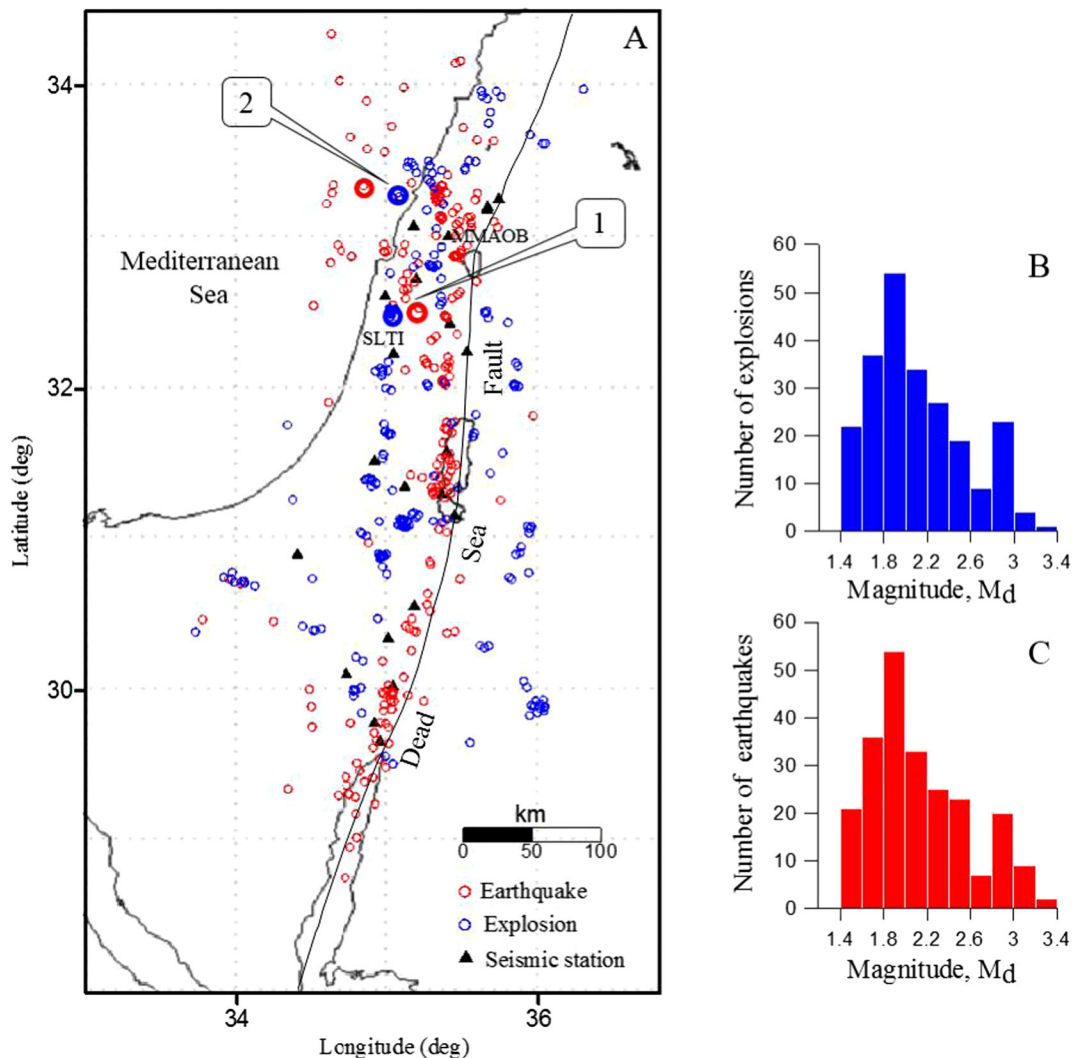
Fig. 1 **a** Location map of explosions, earthquakes, and seismic stations used in this study; the events and stations SLTI and MMAOB used as examples are denoted (positions 1, 2). **b**, **c** Histograms of explosion (*blue*) and earthquake (*red*) duration magnitudes

analysis (Fig. 1b, c). We used only earthquakes shallower than 20 km. The data consist of the vertical components of broadband and short period ISN stations.

The waveforms (stations) were selected by the condition that the seismic event was recorded by at least three calibrated seismic stations located at different epicentral distances and the signal-to-noise ratio exceeds 2. The data processing program JSTAR (Polozov and Pinsky, 2007) was used in the analysis. Available parametric data: local duration magnitude *Md*, epicentral distance, and focal depth, were collected from the seismological bulletin of the Geophysical Institute of Israel. Figure 2 demonstrates a typical example of waveforms at

different stations from an earthquake of 2010/02/06 and from a quarry blast of 2013/02/24, both of the same magnitude, *Md* = 2.0. The distance between the epicenters of these events is about 18 km (see Fig. 1, position 1). It is obvious that the waveforms in this displayed example do not reveal any clear difference between the earthquake and the quarry blast, although sometimes identification of quarry blast seismograms is evident due to longer period surface waves or sonic wave arrivals thus indicating the event blasting character. However, the objective of this study is the comparison of the seismic source effect features of earthquakes and explosions in the frequency domain.
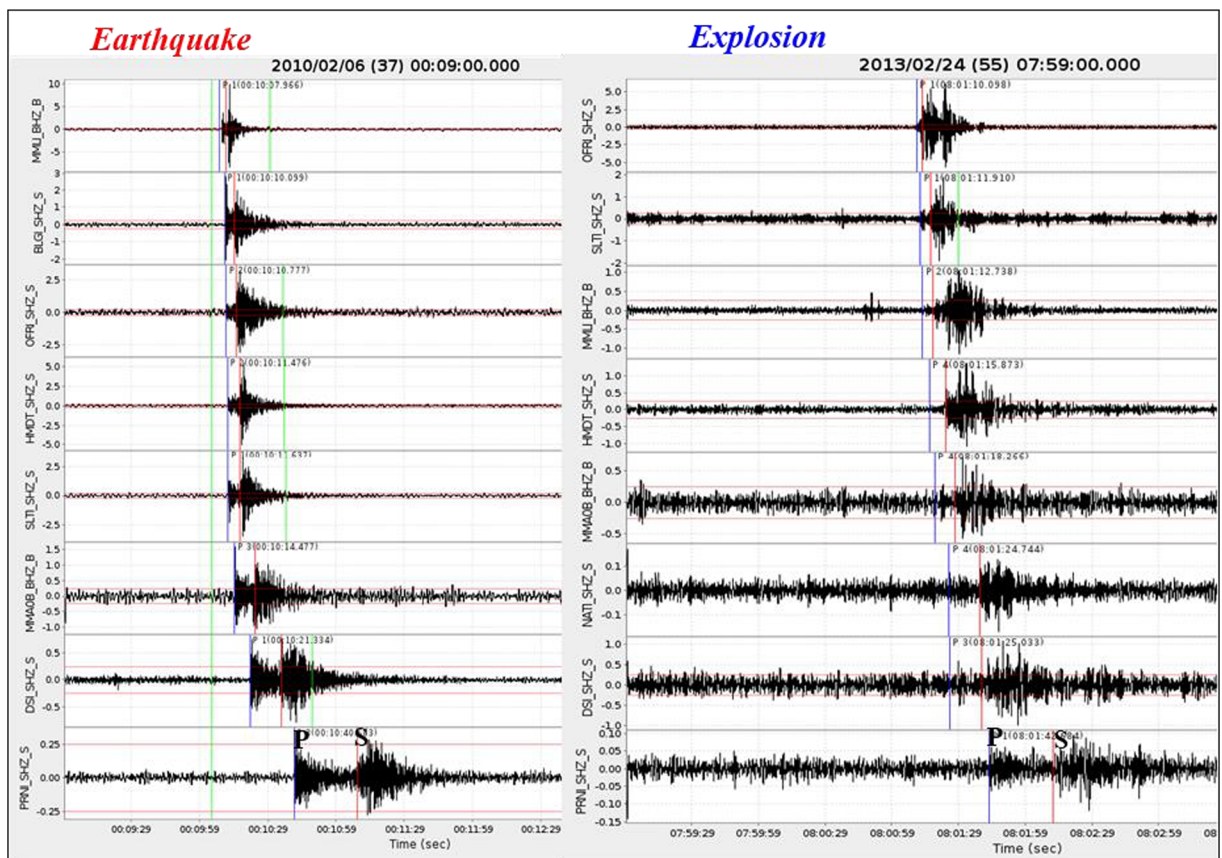
Fig. 2 Sample vertical component seismograms (bandpass filtered 0.5–15 Hz) from an earthquake of 2010/02/06, $Md = 2.0$ and from a quarry blast of 2013/02/24, $Md = 2.0$ (position 1 at

Fig. 1). Traces are sorted according to epicentral distance—from 16 to 240 km for the earthquake and from 18 to 238 km for the explosion. Also the P-wave and S-wave phases are shown

3 Method

3.1 Spectral displacement analysis

We tried to estimate the similarity of the source displacement spectrum of P- and S-waves of an earthquake and an explosion to the theoretical earthquake model. The source parameters of all events were analyzed in accordance with Brune's seismic source model (1970, 1971), using computations of the P- and S-waves displacement Fourier spectra from the vertical component of seismograms. The calculation windows start at the arrival times of P- and S-wave. The P-wave window includes the first group of P phase, increasing with distance from 1.5 to 3 s. The S-wave time window is usually 10–20 s, depending on the distances, and includes the most significant part of the signal energy, as generally accepted for estimation of seismic moment (Brune 1970,1971, Hanks and Wyss 1972, Baumbach

and Borman 2012) The quarry blast S-wave time windows at short distances include also surface Rg waves (actually S + Rg windows). The long S-wave window provided optimal results in separation of earthquakes and explosions.

Then, the corner frequencies, $f_0^I(P)$, $f_0^I(S)$, and the low-frequency spectral amplitudes $\Omega(P)$, $\Omega(S)$ of P- and S-waves are manually measured from calculated displacement spectra for each station record, uncorrected for attenuation, through approximating the spectrum by two lines which refer to constant low-frequency level and high-frequency decay of f^{-2}. The corner frequency is defined as the intersection of low- and high-frequency asymptotes (Brune 1970; Baumbach and Borman 2012; Kiratzi and Louvari 2001; Ashkpour Motolagh and Mostafazadeh 2008; Havskov and Ottemoeller 2010). Records of an earthquake and a quarry blast at station SLTI, located to the south from these events (Fig. 1, position 1), and their P-wave and S-wave displacement

spectra, not corrected prior for attenuation of the seismic waves, are shown in Fig. 3. It is obvious that the displacement spectra of the quarry blast from station SLTI show the lack of high-frequency energy in P-wave and especially in S-wave, and therefore the measured corner frequencies $f_0^{\mathrm{I}}(P)$ and especially $f_0^{\mathrm{I}}(S)$ are lower than those obtained from the earthquake of the same magnitude at the same station.

In addition, we checked a few underwater earthquakes and explosions and found that the displacement spectra of P- and S-wave of the underwater explosions also demonstrate the similar anomalous behavior as distinct from the underwater earthquakes of the same magnitudes (Fig. 4). Note that spectral modulations were found both in S-wave and in P-wave displacement spectra, for some quarry blasts, due to the ripple fired effect, and for some underwater explosions due to the bubbling effect. These modulations were previously observed in the velocity spectra (Gitterman and van Eck, 1993, Gitterman et al., 1998, Gitterman and Shapira, 1994). We also found in some explosions a noticeable scatter of f_0^{I} values at different stations.

3.2 Source parameter estimation

The values of observed corner frequency f_0^{I} and low-frequency spectral amplitude Ω, at distance R, are used to determine the corner frequency f_{0i} and seismic moment M_{0i} at the source from each station i (Brune, 1970, 1971), considering attenuation effect due to geometrical spreading and inelastic attenuation. The principal task is to evaluate the spectra high-frequency decay as the source effect only, excluding the attenuation effect. It was done by utilizing empirical distance correction coefficients for calculating of the corner frequency f_0 and seismic moment M_0 for ISN, following Shapira and Hofstetter (1993) and Ataeva et al. (2015). In this approach, the seismic source parameters, M_0(Nm), f_0 (Hz) and the distance corrections, in general, are described by equations:

$$M_0 = \Omega 4\pi \rho D V^3 \Big/ CF, \qquad D = R^{\alpha} e^{\delta R}, \qquad f_0 = f_0^{\mathrm{I}} e^{\gamma R},$$

with the empirical coefficients:

$\alpha = 0.83$, $\delta = 0.0037$ (S-wave); $\alpha = 1.0$, $\delta = 0.0042$ (P-wave); $\gamma = 0.00043$ (P- and S-wave),

where Ω—observed low-frequency spectral amplitude (m*s), ρ—density, 2700 kg/m^3; V—P-wave (6200 m/s) and S-wave (3600 m/s) velocity; C—free surface amplification, equals 2; F—radiation-pattern

correction factor, $Fs = 0.18$, $F_P = 0.64$; R—hypocentral distance (m), f_0^{I}—corner frequency (Hz) at a station at distance R (Shapira and Hofstetter 1993, Ataeva et al., 2015).

The moment magnitude M_w (Kanamori 1977; Hanks and Kanamori 1979) is calculated as:

$$M_w = 2\Big/ 3(\log_{10} M_0 - 9.1)$$

The corner frequencies $f_0(P)$ and $f_0(S)$ at the source for each event are calculated as the geometrical average of corner frequencies f_{0i} from individual stations i. The f_{0i} values are obtained after the distance correction to the manually measured frequencies f_0^{I}. The averaging reduces the interstation scatter due to possible errors from the manual measuring and the possible local site effect at some stations. For earthquakes, we determined corner frequencies with the standard deviation (in logarithmic units) in the range 0.005–0.116 (average 0.038) for P-wave, and in the range 0.006–0.084 (average 0.035) for S-wave. The standard deviations of explosion corner frequency are estimated between 0.002 and 0.109, the average value $\sigma = 0.040$ (P-wave), and between 0.001 and 0.083, the average value $\sigma = 0.036$ (S-wave). Although the number of used stations in each event is different (3–15 for earthquakes, in most cases 6–8 stations, and 3–8 for explosions, in most cases 4–6 stations), the average standard deviations values σ of corner frequency estimations, for earthquakes and explosions are acceptable and practically identical as required for the confidence of the comparative analysis.
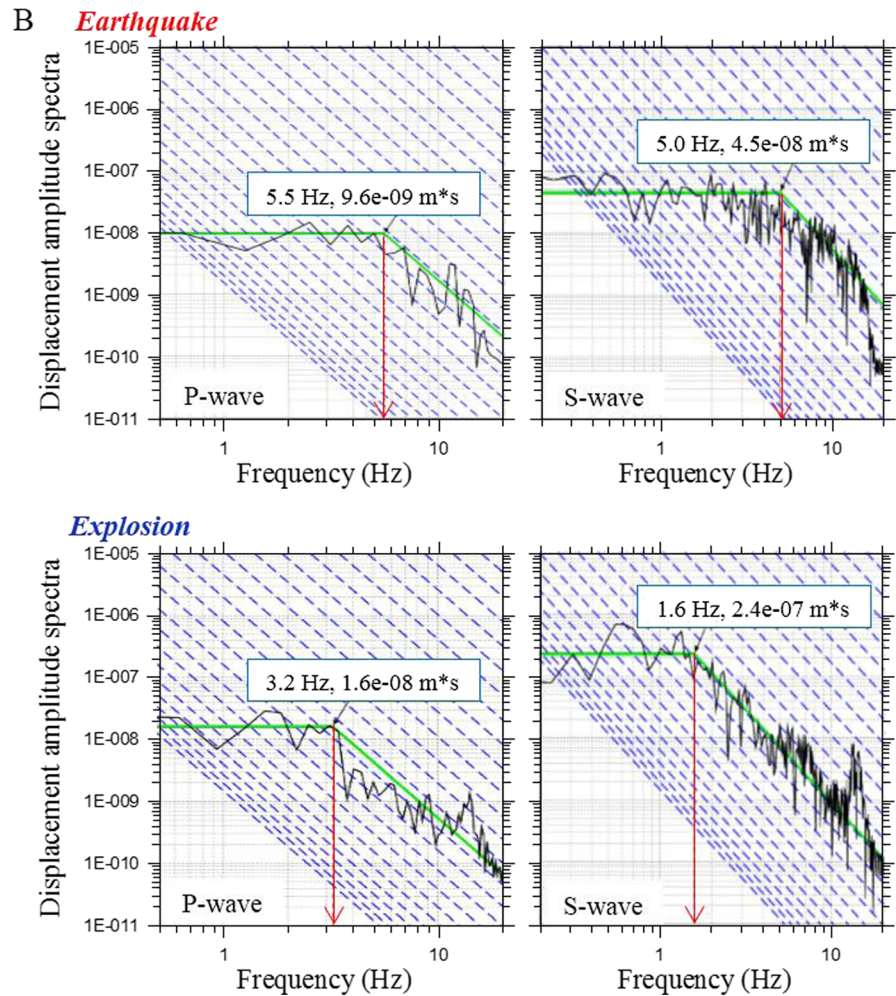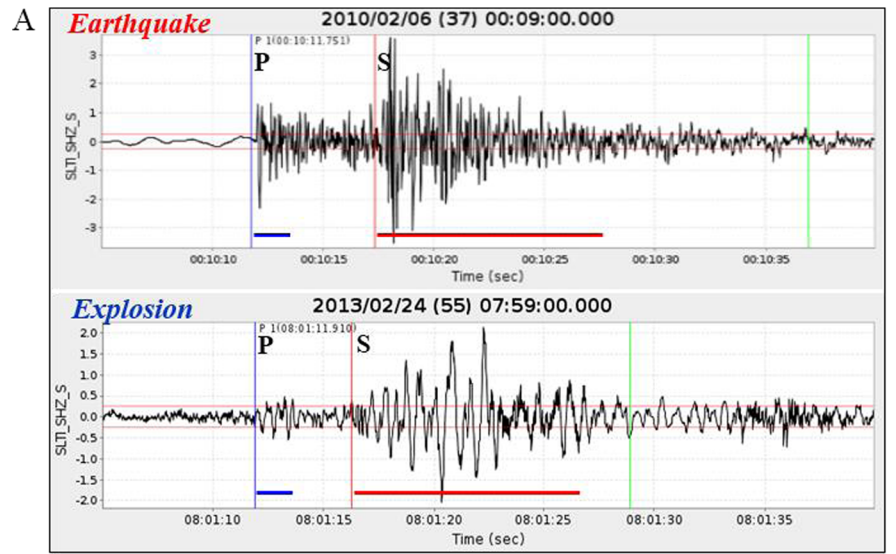
Seismic moment M_0 and moment magnitude M_w from P- and S-wave for all studied events were also calculated by geometrical averaging of values estimated from the individual stations i that recorded the event, thus providing more reliable parameter evaluation. The averaging of source parameter estimates over stations reduces the scatter caused by different station azimuths, especially for P-wave.

4 Results

4.1 Spectral characteristics of quarry blasts in different areas

We have analyzed the spectra of quarry blasts in accordance with quarries location in Israel and adjacent countries and with their duration magnitudes determined by
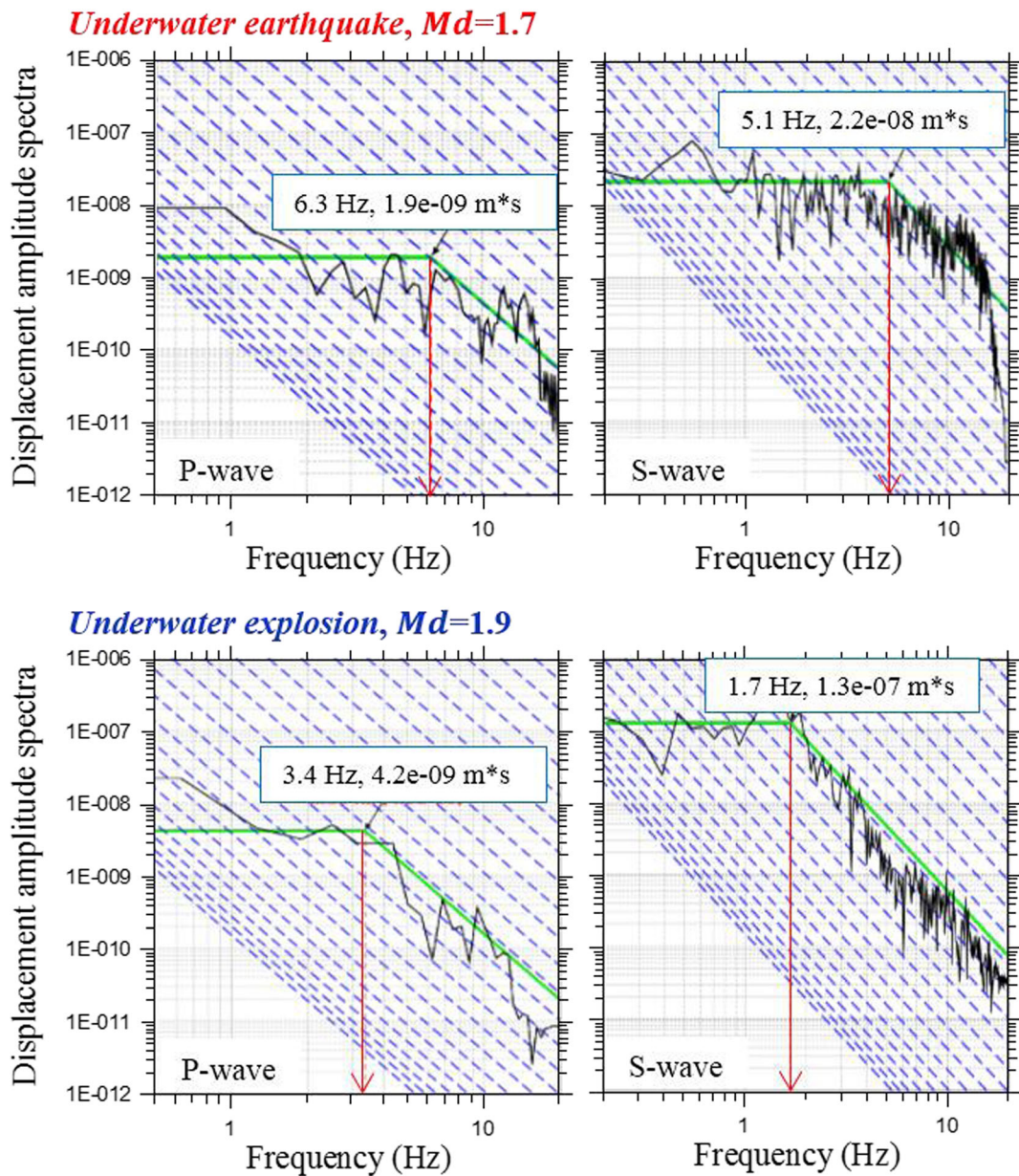
Fig. 4 Uncorrected *P*-wave and *S*-wave displacement spectra (m*s) calculated from seismograms of broad band station MMAOB of an earthquake (2008/03/11, *Md* = 1.7, distance 62 km) and of an explosion (2013/03/11, *Md* = 1.9, 39 km) in E. the Mediterranean Sea (position 2 at Fig. 1). *Green lines* indicate the low-frequency amplitude level and high-frequency decay. The *red line* shows the corner frequency value and *dashed blue lines* show f^{-2} decay. The measured f_0^1 and Ω are shown

the Israeli Seismic Network. We defined three areas, different by the corner frequency $f_0(P)$ and $f_0(S)$ and the duration magnitude M_d range, possibly due to diversity in quarry technology and near-source geology (Fig. 5). For two areas (A, B) prevailing values f_0 are about 2.0 Hz for *S*-wave and about 4.0–4.5 Hz for *P*-wave spectra, when the maximum explosion magnitudes are different. The third area (large quarries in Jordan) is visibly characterized by higher values of the corner frequencies in the displacement spectra: about 3 Hz for *S*-wave and about 5 Hz for *P*-wave and by the maximum magnitude up to 3 (Fig. 5c). We found that spectral displacement corner frequencies of
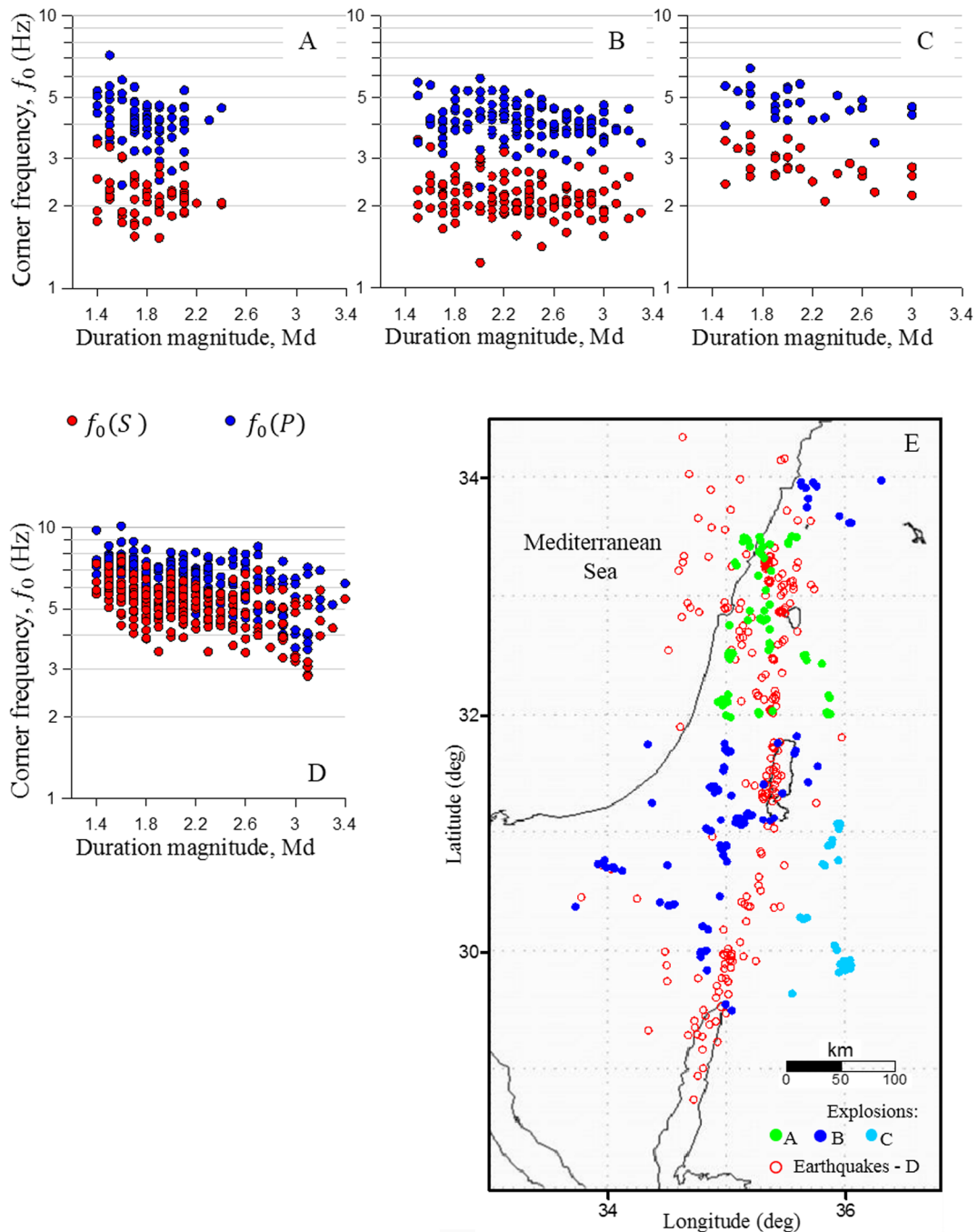
Fig. 5 *S*-wave corner frequency (*red circles*) and *P*-wave corner frequency (*blue circles*) versus the duration magnitude M_d, for explosions in different areas (**a**–**c**) and for earthquakes (**d**); location map of studied earthquakes and explosions at dedicated areas (**e**)

explosions do not depend on the duration magnitude, i.e., the quarry blasts of different magnitudes in Israel have roughly similar corner frequencies. It is important result for practical application of

the discrimination procedure. For comparison, the corner frequencies $f_0(P)$ and $f_0(S)$, for studied earthquakes (Fig. 5d) show a clear dependence of f_0 on duration magnitude M_d.

4.2 Comparison of source spectra parameters for earthquakes and explosion

Average multi-station values M_0, M_w, and f_0 for earthquakes and explosions were used for statistical and comparative analysis, separately for P- and S-waves. Seismic moment versus corner frequency is plotted in Fig. 6 for 226 earthquakes and 230 explosions, with histogram distribution of the corner frequency for P- and S-waves. The analysis shows significantly lower corner frequencies f_0 of explosions than earthquakes, especially for S-wave displacement spectra. Seismic moments M_0 of earthquakes and explosions, located in the same range, are not separated and cannot be used as a discriminant (Fig. 6a, b). Presented data suggest also the lower stress-drop for explosions compared to earthquakes. The stress drop concept has no meaning for

explosions and qualified here as if interpreted for an earthquake. Nonetheless, determination of stress-drop values and their analysis as discriminant is beyond the scope of this study. Figure 6 shows a minor overlap in the corner frequency distributions for earthquakes and explosions, the overlap is larger for P-wave values. In general, the shift $f_0(P)$ relative to $f_0(S)$ is obviously higher for explosions than for earthquakes.

4.3 Corner frequency ratio $f_0(P)/f_0(S)$ and discriminant formulation

In accordance with the earthquake source model and following Hanks and Wyss (1972), Molnar et al. (1973), later by Watanabe et al. (1996) and by Tusa and Gresta (2008), it was found that $f_0(P) > f_0(S)$. In Israel for earthquakes of magnitude $M_w = 2.7–5.6$ an average empirical
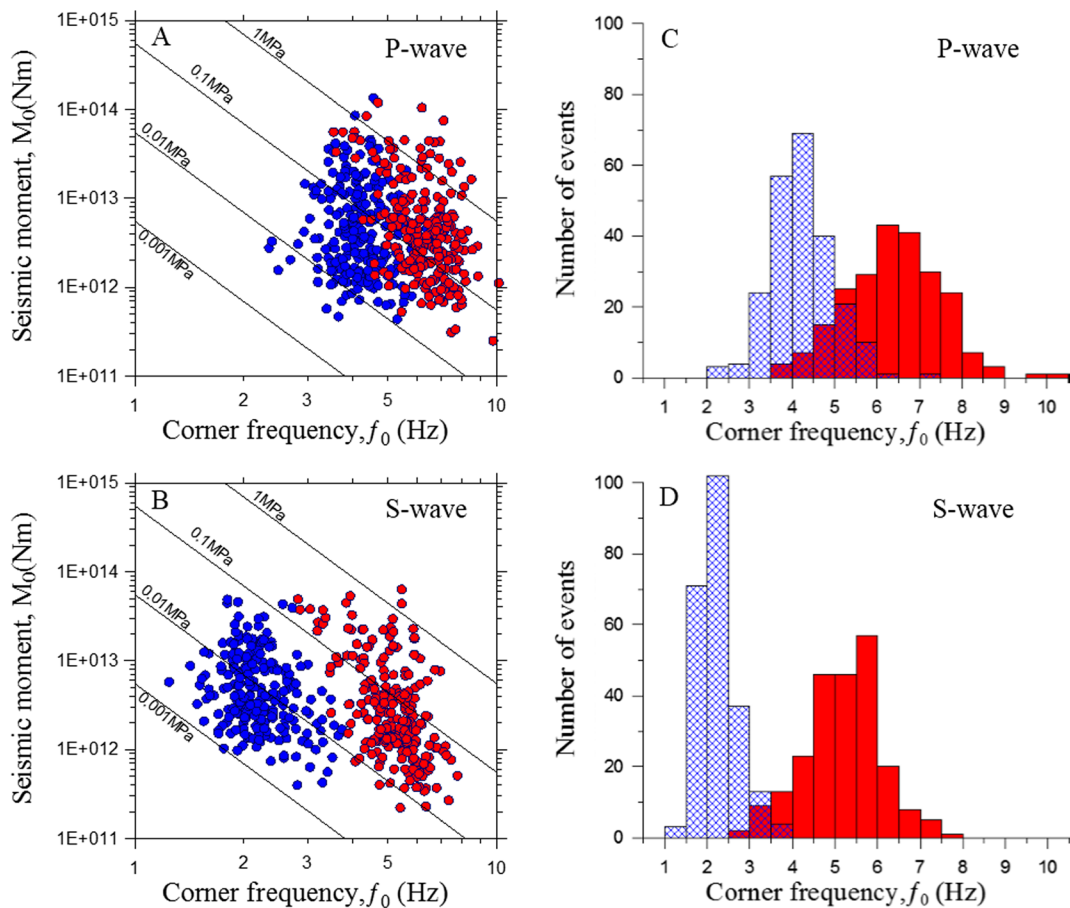

Fig. 6 Seismic moment M_0 versus corner frequency f_0 for studied earthquakes (*red circles*) and explosions (*blue circles*) obtained from P-wave (**a**) and S-wave (**b**). The *solid lines* indicate the constant stress drop in accordance with the Brune's source model.

Histograms of the corner frequency for all studied earthquakes (*red*) and explosions (*blue cross*) were obtained from P-wave (**c**) and S-wave (**d**) spectra

ratio was obtained: $f_0(P)/f_0(S) = 1.24$ (Ataeva et al., 2015). Based on the conducted analysis presented in Fig. 6, the ratio between $f_0(P)$ and $f_0(S)$ is larger for explosions than for earthquakes. This result assumes an ability for discrimination. Figure 7a demonstrates the comparison between corner frequencies estimated from P- and S-waves for studied earthquakes and explosions. The average ratios are obtained: $f_0(P)/f_0(S) = 1.23$ for 226 earthquakes with standard deviation of 0.18, coefficient of determination of 0.98 and $f_0(P)/f_0(S) = 1.86$ for 230 explosions with standard deviation of 0.27 and coefficient of determination of 0.97. The ratios $f_0(P)/f_0(S)$ do not depend on estimated moment magnitude M_w, and distributed for earthquakes in the range 1.05–1.48, which is clearly different from the range 1.49–2.85 for explosions, with a suggested threshold value about 1.48 (Fig. 7b). The empirical threshold value was derived as the average of the largest earthquake and the smallest explosion ratios $f_0(P)/f_0(S)$. The observed full separation of earthquakes and explosions was obtained for the selected dataset; no event was excluded as an outlier. Some earthquakes and explosions show very close ratios, within measurement errors. Some overlap for another event selection can be expected.

The presented analysis demonstrates feasibility of the $f_0(P)/f_0(S)$ ratio as an effective discriminant, separating earthquakes and explosions. The significant scatter in the explosion corner frequency ratios (Fig. 7b) might be explained by different quarry technology feature (variable ripple firing delays, number of delays) and by local near-source geology. The effect of near-source

(explosion) material properties on the spectral characteristics (spectral slope and corner frequency) of P-wave was demonstrated by Ford et al. (2011) and Walter et al. (1995). It should be noted that most of small $f_0(P)/f_0(S)$ are obtained from displacement spectra of the quarry blasts in Jordan, which are characterized by higher corner frequency values (Fig. 5c).

The Corner Frequency Discriminant (CFD), which we propose, includes estimations of all corner frequencies from the individual stations of the event from P- and S-waves, then corrected for distance, and finally computation of the discriminant with the averaged multi-station values $f_0(P)$ and $f_0(S)$:

$$CFD = f_0(P) \Big/ f_0(S).$$

5 Discussion and conclusions

The P- wave and S-wave displacement spectra from local earthquakes and explosions with similar magnitudes were analyzed and compared in this study. We explored 2430 digital records of the Israeli Seismic Network (ISN) from 456 events (226 earthquakes and 230 explosions) of magnitudes $M_d = 1.4$–3.4. The short period and broad band vertical component seismograms were used in the analysis.

This study concluded that the low-magnitude shallow earthquakes and the explosions in Israel demonstrate significant differences in their spectral properties.
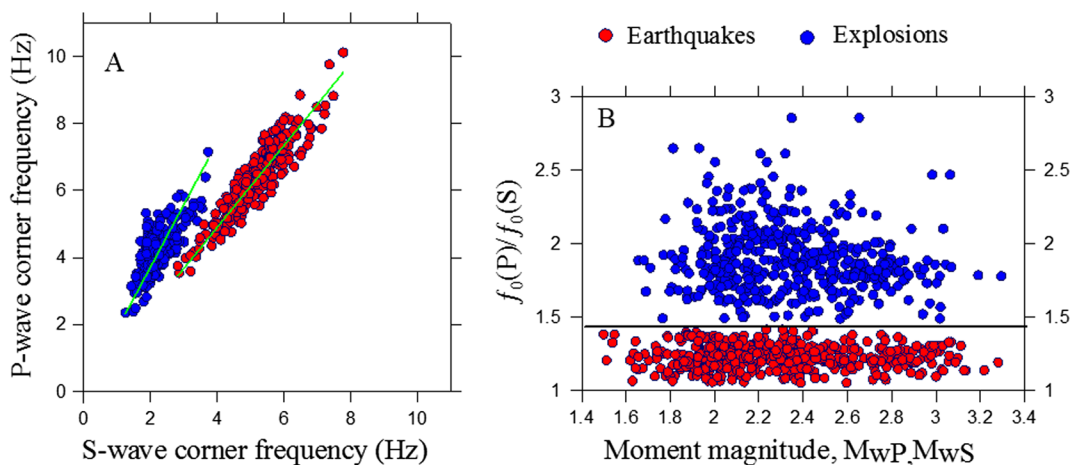

Fig. 7 **a** Corner frequency $f_0(P)$, determined from P-wave analysis, versus corner frequency $f_0(S)$, determined from S-wave analysis. The *green solid lines* are the least-squares fits to the data. **b** Ratio between the corner frequencies versus moment magnitude M_w estimated from P- and S-wave. The *black line* represents the empirical discrimination threshold value ~1.48 for Israel

We focused on the corner frequency only, assuming the standard model of f^{-2} spectral fall (Brune. 1970, 1971), and did not analyzed the change in slope of the high-frequency fall-off because of the complexity of explosion and earthquake spectral shapes. The corner frequency from displacement spectra is the most important information about the seismic source type that can be used for discrimination. To obtain the source corner frequency, we applied the empirical attenuation parameter (Ataeva et al., 2015) that characterizes the propagation effect in the medium and provides reliable results similar to those of Brune's method. We used for measurements all available stations (3–15 for earthquakes and 3–8 for explosions), in some cases with one recorded phase. Although uncertainties in manual measuring of the corner frequencies can be quite large, yet, the obtained relatively small standard deviations of geometrical average of corner frequencies for earthquakes and explosions suggest that our approach is valid.

The quarry blast S-wave windows, used in our study, at short distances may include Rg phase. The amplitude of this fundamental mode Rayleigh wave is strongly depth dependent, it is often observed with large amplitudes in near surface events such as quarry blasts (e.g., McLaughlin et al. 2004) and not usually observable in earthquakes with depths greater than a few km. We found that including Rg large amplitudes in the calculating of S-wave displacement spectra (actually S + Rg waves) has 15 % lowering effect on the observed corner frequencies, staying within obtained standard deviation (logarithmic units) of averaged corner frequencies for each event. Since we use available stations from the different distances, the corner frequencies for quarry blasts at the larger distances more often obtained from S-wave.

Our results show that the corner frequencies of P-wave and especially S-wave source displacement spectra of quarry blasts are lower than obtained from earthquakes of the same magnitudes, due to losses of the high frequency seismic energy, caused by wave propagation in near-surface soft sediment layers. Many researchers observed this effect in seismograms of quarry blasts (Taylor et al., 1988, Bennett and Murphy, 1986, Su et al., 1991, Gitterman, et al., 1998) and in P-wave displacement spectra (Shearer and Allmann, 2007, Allmann, et al., 2008). However, we observed in the corner frequency distributions of earthquakes and explosions an overlap (larger for P-waves than for S-waves), which does not allow completely separate explosions from earthquakes. We demonstrated that prevailing values of corner

frequency of all selected explosions are about 2.0–2.5 Hz for S-wave and about 4.0–4.5 Hz for P-wave spectra, i.e., the quarry blasts of different magnitudes have roughly the same corner frequencies.

We found that the ratio between $f_0(P)$ and $f_0(S)$ is higher for explosions than for earthquakes. Ratios $f_0(P)/f_0(S)$ between the corner frequencies of P-waves and S-waves are distributed in the range 1.05–1.48 (average 1.23) for earthquakes, and in the range 1.49–2.85 (average 1.86) for explosions. We used the difference in these ratios as an effective discrimination parameter which is not dependent on moment magnitude M_w. The presented new discriminant is more closely related to source than to depth type, because is based on the ratio of P to S corner frequencies, but not on the S + Rg window corner frequency alone.

However, we can suggest that scatter in the explosion corner frequencies ratios might be caused not only by the different technologies of quarries and local near-source geology but also by the ambiguity of S or S + Rg corner frequency determination.

The proposed discrimination parameter, $CFD = f_0(P)/f_0(S)$ is formed from corner frequencies estimated for individual stations, then corrected for distance, finally the ratio is calculated from the averaged values $f_0(P)$ and $f_0(S)$. This is a new approach providing effective multi-station discrimination between low-magnitude shallow earthquakes and explosions in Israel. The same method is likely to be applicable in other regions with similar quarry technology. We may expect a different discriminant value for different detonation conditions.

References

Allmann BP, Shearer PM, Hauksson E (2008) Spectral discrimination between quarry blasts and earthquakes in southern California. Bull Seis Soc Am 98:2073–2079

Anderson DN, Walre WR, Fagan DK, Mercier TM, Taylor SR (2009) Regional multistation discriminants: magnitude, distance, and amplitude corrections, and sources of error. Bull Seis Soc Am 99(2A):794–808

Arrowsmith SJ, Arrowsmith MD, Hedlin MAH, Stump B (2006) Discrimination of delay-fired mine blasts in Wyoming using an automatic time-frequency discriminant. Bull Seis Soc Am 96(6):2368–2382

Arrowsmith SJ, Hedlin MAH, Arrowsmith MD, Stump B (2007) Identification of delay-fired mining explosions using seismic arrays: application to the PDAR array in Wyoming, USA. Bull Seis Soc Am 97(3):989–1001

Ashkpour Motolagh S, Mostafazadeh M (2008) Source parameters of the Mw 5.8 Fin (south of Iran) earthquake of March 25, 2006. World Appl Sci J 4:104–115

Ataeva G, Shapira A, Hofstetter A (2015) Determination of source parameters for local and regional earthquakes in Israel. J Seismol 19(2):389–401

Baumbach M, Borman P (2012) Determination of source parameters from seismic spectra. New Manual of Seismological Observatory practice 2 (NMSOP-2) (pp. 1–7). Deutsches Geo Forschugs Zentrum GFZ, Potsdam

Bennett T, Murphy J (1986) Analysis of seismic discrimination capabilities using regional data from western United States events. Bull Seis Soc Am 76(4):1069–1086

Brune J (1970) Tectonic stress and spectra of seismic shear waves from earthquakes. J Geophys Res 75:4997–5009

Brune JN (1971) Correction. J Geophys Res 76:5002

Carr DB, Garbin HD (1998) Discriminating ripple-fired explosions with high-frequency (>16 Hz) data. Bull Seis Soc Am 88(4):963–972

Chapman M (2008) Seismological discrimination of blasts and natural earthquakes. Workshop on Blasting, West Virginia

Dahy SA, Hassib GH (2010) Spectral discrimination between quarry blasts and microearthquakes in Southern Egypt. Res JEarth-Sci 2:01–07

Ford SR, Walter WR, Ruppert SD, Matzel EM, Hauk TF, Gok R (2011) Toward an empirically-based parametric explosion spectral model in Proceedings of the 2011 Monitoring Research Review: Ground-Based Nuclear Explosion Monitoring Technologies, DE-AC52-07NA27344/LL08.

Gitterman Y, Shapira A (1994) Spectral characteristics of seismic events off the coast of the Levant. Geophys J Int 116:485–497

Gitterman Y, van Eck T (1993) Spectra of quarry blasts and microearthquakes recorded at local distances in Israel. Bull Seis Soc Am 83:1799–1812

Gitterman Y, Pinsky V, Shapira A (1998) Spectral classification methods in monitoring small local events by the Israel seismic network. J Seismol 2(3):237–256

Hanks T, Kanamori H (1979) A moment magnitude scale. J Geophys Res 84:2348–2350

Hanks T, Wyss M (1972) The use of body-wave spectra in the determination of seismic-source parameters. Bull Seis Soc Am 62(2):561–589

Hartse HE, Phillips WS, Fehler MC, House LS (1995) Single station spectral discrimination using coda waves. Bull Seis Soc Am 85(5):1464–1474

Havskov J, Ottemoeller L (2010) Routine data processing in earthquake seismology. Springer, Dordrecht, p 347. doi:10.1007/978-90-481-8697-6

Hedlin MA, Minster JB, Orcutt JA (1990) An automatic means to discriminate between earthquakes and quarry blasts. Bull Seis Soc Am 80(6B):2143–2160

Kanamori H (1977) The energy release in great earthquakes. J Geophys Res 82:2981–2987

Kim WY, Simpson DW, Richards PG, Smith AT (1993) Discrimination of explosions from simultaneous mining blasts. Bull Seis Soc Am 83(1):160–179

Kim WY, Simpson DW, Richards PG (1994) High-frequency spectra of regional phases from earthquakes and chemical explosions. Bull Seis Soc Am 84(5):1365–1386

Kiratzi A, Louvari E (2001) Source parameters of the Izmit-Bolu 1999 (Turkey) earthquake sequences from teleseismic data. Ann Geofis 44:33–47

McLaughlin KL, Bonner JL, Barker T (2004) Seismic source mechanisms for quarry blasts: modeling observed Rayleigh and Love wave radiation patterns from a Texas quarry. Geoph J Int 156(1):79–93

Molnar P, Tucker B, Brune J (1973) Corner frequencies of P and S waves models of earthquake sources. Bull Seism Soc Amer 63:2091–2104

Morozov AN (2008) Method of identification of explosive seismicity on territories of the Arkhangelsk region. Institute of Ecological Problem in the North of UB RAS, Arkhangelsk

Plafcan D, Sandvol E, Seber D, Barazangi M, Ibenbrahim A, Cherkaoui T (1997) Regional discrimination of chemical explosions and earthquakes: a case study in Morocco. Bull Seis Soc Am 87:1126–1139

Polozov A, Pinsky V (2007) New software for seismic network and array data processing and joint seismological data base. GII report 546/307/07

Shapira A, Hofstetter A (1993). Source parameters and scaling relationship of earthquakes in Israel. Teconophysics 217:217–226

Shearer PM, Allmann BP (2007) Spectral studies of shallow earthquakes and explosions in Southern California, in Proceedings of the 29th Monitoring Research Review: Ground-Based Nuclear Explosion Monitoring Technologies, p 656-662

Smith AT (1993) Discrimination of explosions from simultaneous mining blasts. Bull Seis Soc Am 83:160–179

Su F, Aki K, Biswas NN (1991) Discriminating quarry blasts from earthquakes using coda waves. Bull Seis Soc Am 81(1):162–178

Taylor SR, Sherman NW, Denny MD (1988) Spectral discrimination between NTS explosions and western United States earthquakes at regional distances. Bull Seis Soc Am 78(4):1563–1579

Tusa G, Gresta S (2008) Frequency-dependent attenuation of P waves and estimation of earthquake source parameters in southeastern Sicily, Italy. Bul Seis Soc Amer 98(6):2772–2794

Walter WR, Mayeda KM, Patton HJ (1995) Phase and spectral ratio discrimination between NTS earthquakes and explosions; part I, empirical observation. Bull Seis Soc Am 85(4):1050–1067

Watanabe K et al (1996) Source characteristics of small to moderate earthquakes in the Kanto Region, Japan: application of a new definition of the S-wave time window length. Bul Seis Soc Amer 86(5):1284–1291

Wuster J (1993) Discrimination of chemical explosions and earthquakes in central Europe - a case study. Bul Seis Soc Amer 83:1184–1212

Wyss M, Hanks T (1971) Comparison of P-wave spectra of underground explosions and earthquakes. J Geoph Res 76:2716–2729